1-16-2024

Hormonal basis of sex differences in anesthetic sensitivity

Andrzej Z Wasilczuk
University of Pennsylvania

Cole Rinehart
University of Pennsylvania

Adeeti Aggarwal
University of Pennsylvania

Martha E Stone
University of Pennsylvania

George A Mashour
University of Michigan - Ann Arbor

See next page for additional authors

PNAS RESEARCH ARTICLE | NEUROSCIENCE OPEN ACCESS

Hormonal basis of sex differences in anesthetic sensitivity

Andrzej Z. Wasilczuk[a,b,c], Cole Rinehart[a,b], Adeeti Aggarwal[a,b,d], Martha E. Stone[a,b,d], George A. Mashour[e], Michael S. Avidan[f], Max B. Kelz[a,b,d,g,1], Alex Proekt[a,b,d,g,1], and ReCCognition Study Group[a,e,f,2]

Edited by Donald Pfaff, Rockefeller University, New York, NY; received July 27, 2023; accepted November 20, 2023

General anesthesia—a pharmacologically induced reversible state of unconsciousness—enables millions of life-saving procedures. Anesthetics induce unconsciousness in part by impinging upon sexually dimorphic and hormonally sensitive hypothalamic circuits regulating sleep and wakefulness. Thus, we hypothesized that anesthetic sensitivity should be sex-dependent and modulated by sex hormones. Using distinct behavioral measures, we show that at identical brain anesthetic concentrations, female mice are more resistant to volatile anesthetics than males. Anesthetic sensitivity is bidirectionally modulated by testosterone. Castration increases anesthetic resistance. Conversely, testosterone administration acutely increases anesthetic sensitivity. Conversion of testosterone to estradiol by aromatase is partially responsible for this effect. In contrast, oophorectomy has no effect. To identify the neuronal circuits underlying sex differences, we performed whole brain c-Fos activity mapping under anesthesia in male and female mice. Consistent with a key role of the hypothalamus, we found fewer active neurons in the ventral hypothalamic sleep-promoting regions in females than in males. In humans, we demonstrate that females regain consciousness and recover cognition faster than males after identical anesthetic exposures. Remarkably, while behavioral and neurocognitive measures in mice and humans point to increased anesthetic resistance in females, cortical activity fails to show sex differences under anesthesia in either species. Cumulatively, we demonstrate that sex differences in anesthetic sensitivity are evolutionarily conserved and not reflected in conventional electroencephalographic-based measures of anesthetic depth. This covert resistance to anesthesia may explain the higher incidence of unintended awareness under general anesthesia in females.

sex differences | hormones | behavior | EEG | whole brain c-Fos imaging

Significance

Half of all surgical patients receiving anesthesia are females. Anesthetics affect sexually dimorphic brain regions involved in sleep and arousal. Yet, sex differences and the effects of sex hormones on anesthetic sensitivity have not been systematically explored. We demonstrate that the female brain in mice and humans is resistant to the hypnotic effects of volatile anesthetics. Sex differences in anesthetic sensitivity are largely due to acute effects of sex hormones. Despite clear behavioral differences in anesthetic sensitivity, sex differences are not discernable in clinically used cortical electroencephalographic recordings. In contrast, subcortical sites exhibit sexually dimorphic activity patterns under anesthesia. This covert resistance to anesthetics may explain the higher incidence of awareness under anesthesia in females.

General anesthetics transformed modern medicine by allowing life-saving surgeries to be performed safely over 300 million times each year (1). While states of natural sleep and anesthesia are clearly distinct, an increasing body of evidence across species strongly implies that anesthetics act in part by modulating activity within the endogenous sleep-wake circuitry (2–6). Mechanistically diverse anesthetics activate neurons in the sleep-promoting nuclei and inhibit wake-promoting neurons (2, 7–10). Many nuclei that control the state of arousal are located in the hypothalamus (11, 12). Interestingly, the hypothalamic nuclei involved in the control of sleep and wakefulness are highly sexually dimorphic structures (13–20), modulated by sex hormones (21). This suggests that the effects of anesthetics may be sex and hormone dependent.

The clinical literature on sex differences in anesthetic sensitivity is controversial. Early work suggested that males and females have the same sensitivity to volatile anesthetics (22). In contrast, newer studies focusing on intraoperative awareness without recall (23) found a nearly threefold increase in the likelihood of awareness in female patients. Female sex was found to be a risk factor for awareness associated with postoperative recall in some studies (24–33) but not in others (34–36). A recent meta-analysis concluded that females are at higher risk of awareness with or without recall and emerge from the state of anesthesia faster than males (37).

However, several important confounders dramatically limit the interpretability of these clinical data. Most studies on anesthetic awareness were not specifically designed to identify sex differences. While some studies examined the effect of the menstrual cycle on anesthetic sensitivity (38, 39), no causal manipulations linking the hormonal state to anesthetic sensitivity were performed. Further, clinical studies cannot exclude the possibility that differences in drug distribution and elimination contribute to the apparent sex differences in the incidence of awareness. Finally, heterogeneous patient populations undergoing different surgeries under different anesthetic regimens could have contributed to the inconsistency of the clinical data. Thus, existing clinical trials are ill equipped to demonstrate or mechanistically explain the potentially sexually dimorphic responses to general anesthetics.

Author contributions: A.Z.W., G.A.M., M.S.A., M.B.K., and A.P. designed research; A.Z.W., C.R., A.A., M.E.S., G.A.M., M.S.A., M.B.K., A.P., and R.S.G. performed research; A.Z.W., A.A., M.E.S., and A.P. analyzed data; A.Z.W., C.R., A.A., M.E.S., G.A.M., M.S.A., M.B.K., and A.P. edited the paper; and A.Z.W., M.B.K., and A.P. wrote the paper.

The authors declare no competing interest.

This article is a PNAS Direct Submission.

[1]To whom correspondence may be addressed. Email: kelzma@pennmedicine.upenn.edu or proekt@gmail.com.

[2]A complete list of the ReCCognition Study Group can be found in the *SI Appendix*.

This article contains supporting information online at https://www.pnas.org/lookup/suppl/doi:10.1073/pnas.2312913120/-/DCSupplemental.

Published January 8, 2024.

Historically, sex has been largely ignored in animal studies for anesthesia research despite contrasting clinical evidence (40, 41). Conflicting results have been previously reported using rodents as a model organism for studying sex differences in anesthetic sensitivity (42–45). A common explanation for these disparities has been cyclic fluctuations of sex hormones (44–48). Despite recent efforts to elucidate sex and hormonal effects on anesthetic sensitivity, pharmacokinetic confounds complicate the interpretations of many studies. Whether sex-dependent brain circuit maturation and/or post-pubertal sex hormone levels affect steady-state anesthetic sensitivity remains largely unknown.

To address this critical knowledge gap, we explicitly test the influence of sex and sex hormones on sensitivity to volatile anesthetics in mice. We measured multiple behavioral endpoints for anesthetic sensitivity across four different volatile anesthetics in male and female mice. Direct measurements of brain anesthetic concentration eliminated potential pharmacokinetic confounds. We altered the postpubertal hormonal state of mice by castration and oophorectomy, by exogeneous administration of sex hormones, and by pharmacological modulation of the enzymes critical for hormone biosynthesis. These experiments yield an unequivocal conclusion that the female brain is more resistant to anesthetics and that this sex difference in anesthetic sensitivity is bidirectionally modulated by acute effects of testosterone. Analysis of multiple behavioral and neurocognitive measures in healthy human volunteers who underwent a precisely controlled anesthetic exposure in the absence of surgical stimuli (49) confirmed that human females are also more resistant to volatile anesthetics. Interestingly, the electroencephalogram (EEG) failed to reveal sex differences in mice or humans. The lack of sex differences in cortical activity was corroborated by whole brain c-Fos expression mapping in mice under anesthesia. In contrast, multiple hypothalamic sleep-promoting structures exhibited lower levels of c-Fos expression under anesthesia in female mice. These results suggest a hypothalamic origin of the increased anesthetic resistance in females. Interestingly, this increased resistance is not readily detectable in the EEG.

Results

The Female Brain is More Resistant to the Hypnotic Effects of Anesthetics. To determine whether sex differences in anesthetic sensitivity exist, we used the righting reflex to generate induction and emergence dose–response curves (Fig. 1*A*) for isoflurane in male and female mice. The mean EC_{50} for induction was significantly higher in females (0.90% atm., 95% CI [0.88 to 0.92]) compared to males (0.68% atm., 95% CI [0.66 to 0.70]). The dose–response curve for emergence was also significantly right-shifted in females relative to males (EC_{50} female emergence 0.66% atm., 95% CI [0.58 to 0.73] vs. EC_{50} male emergence 0.37% atm., 95% CI [0.34 to 0.41]). Similar differences in sensitivity were observed for all tested volatile anesthetics: sevoflurane, halothane, and desflurane (*SI Appendix*, Table S1). Female mice took longer to become anesthetized (Fig. 1*B*) and emerged faster (Fig. 1*C*) than male mice [induction times: WT M (wild-type male) 224 ± 66 s (mean ± SD) (226 s [157 to 278] (median [IQR])), WT F (wild-type female) 314 ± 69 s (318 s [255 to 378]], $P = 0.0080$, unpaired *t* test; emergence times: WT M 419 ± 252 s (472 s [253 to 668]), WT F 257 ± 139 s (224 s [146 to 347]), $P = 0.019$, unpaired *t* test). These data suggest that females are more resistant to the hypnotic effects of volatile anesthetics.

While the righting reflex is a well-established measure of anesthetic effects in rodents (50), it has some notable limitations (51, 52). To eliminate these potential confounds, we confirmed our results using the adhesive sticker removal test (Fig. 1*D*). Removal of the adhesive sticker from the snout signifies both sensory awareness of the stimulus and requires a coordinated motor response (50). Consistent with our righting reflex assessment of anesthetic sensitivity, female mice successfully removed the sticker faster than males (WT F 242 ± 177 s (mean ± SD) (181 s [121 to 308] (median [IQR])), WT M 483 ± 235 s (421 s [294 to 687]), $P = 0.019$, unpaired *t* test) after identical exposures to isoflurane anesthesia. Thus, independent behavioral measures converge on the fact that female mice are more resistant to isoflurane than males.

To differentiate between potential pharmacokinetic and pharmacodynamic mechanisms, we investigated sex differences in anesthetic sensitivity at pharmacokinetic steady state (53, 54). Righting reflex assessments were made every 3 min during the final 2 h of a 4-h isoflurane exposure (0.6% atm) delivered in a hermetically sealed and temperature controlled chamber (Fig. 1*E*). Previous studies using this apparatus established that isoflurane concentration in the brain reaches steady state within 10 min (55). Consistent with the results in Fig. 1 *A*–*D*, at steady state (Fig. 1*F*), the group of female mice was more likely than the group of males to exhibit intact righting reflex (WT F 0.64 ± 0.05 (mean ± SD) (0.64 [0.60 to 0.67] (median [IQR])), WT M 0.44 ± 0.06 (0.46 [0.40 to 0.48]), $F_{(1,240)} = 145.6$, $P < 0.0001$, 2-way ANOVA, Sex by Time). Moreover, when individual responses were averaged across time, the mean individual responsiveness (Fig. 1*G*) in WT F was also significantly higher as compared to WT M (WT M 0.44 ± 0.19 (mean ± SD) (0.45 [0.31 to 0.61] (median [IQR])), WT F 0.63 ± 0.15 (0.65 [0.50 to 0.73]), $P = 0.0011$, unpaired *t* test). Critically, there was no detectable difference in the brain isoflurane concentration (Fig. 1*H*) between females (241.2 ± 25.6 μg-iso/g-brain tissue (mean ± SD) (234 [218 to 268] (median [IQR])) and males (251.8 ± 38.2 μg-iso/g-brain tissue (241 [222 to 287]) during identical anesthetic exposure ($P = 0.62$, unpaired *t* test). The mean time (across groups) between end of isoflurane exposure and the brain being flash-frozen was 40.4 ± 6.1 s (mean ± SD) (41.5 s [36.5 to 44.25] (median [IQR]) respectively. No differences were observed between time to cervical dislocation, time to flash-freeze brain, or mouse core temperature between groups ($F_{(1,8)} = 0.00037$, $P = 0.985$, 2-way ANOVA, Sex by Harvest Parameters). Thus, sex differences in anesthetics sensitivity cannot be explained by pharmacokinetic differences in drug distribution. This, in turn, implies the existence of divergent effects of anesthetics on the male and female brain.

To determine whether sex differences in anesthetic sensitivity are also observed in humans, we reanalyzed data collected from the ReCCognition trial (NCT01911195). In this trial, 30 healthy human volunteers (12 women and 18 men, 22 to 40 y old) were given isoflurane at 1.3 age-adjusted MAC (corresponding to 1.7 to 1.9%) for 3 h. EEG was recorded throughout the anesthetic exposure, and serial neurocognitive exams were performed at baseline prior to anesthetic exposure, immediately upon emergence from anesthesia, and every 30 min over the ensuing 3 h (56, 57) As with mice, human females regained the ability to follow auditory cues, signifying emergence from anesthesia (Fig. 1*I*), faster than males (Human F: 28.8 ± 8.5 min (mean ± SD) (26.4 min [23.9 to 32.3] (median [IQR]), Human M: 44.6 ± 13.8 min (41.0 [34.4 to 55.1]), $P = 0.0017$, unpaired *t* test). To determine whether restoration of cognition after anesthesia also exhibits sex differences, we utilized the psychomotor vigilance test. The psychomotor vigilance test measures cognitive awareness and sustained attention (57). We found that females performed faster (Fig. 1*J*) ($F_{(1,28)} = 7.823$, $P = 0.0092$, 2-way ANOVA, Sex by Time) and more accurately (Fig. 1*K*) ($F_{(1,28)} = 12.16$, $P = 0.0016$, 2-way

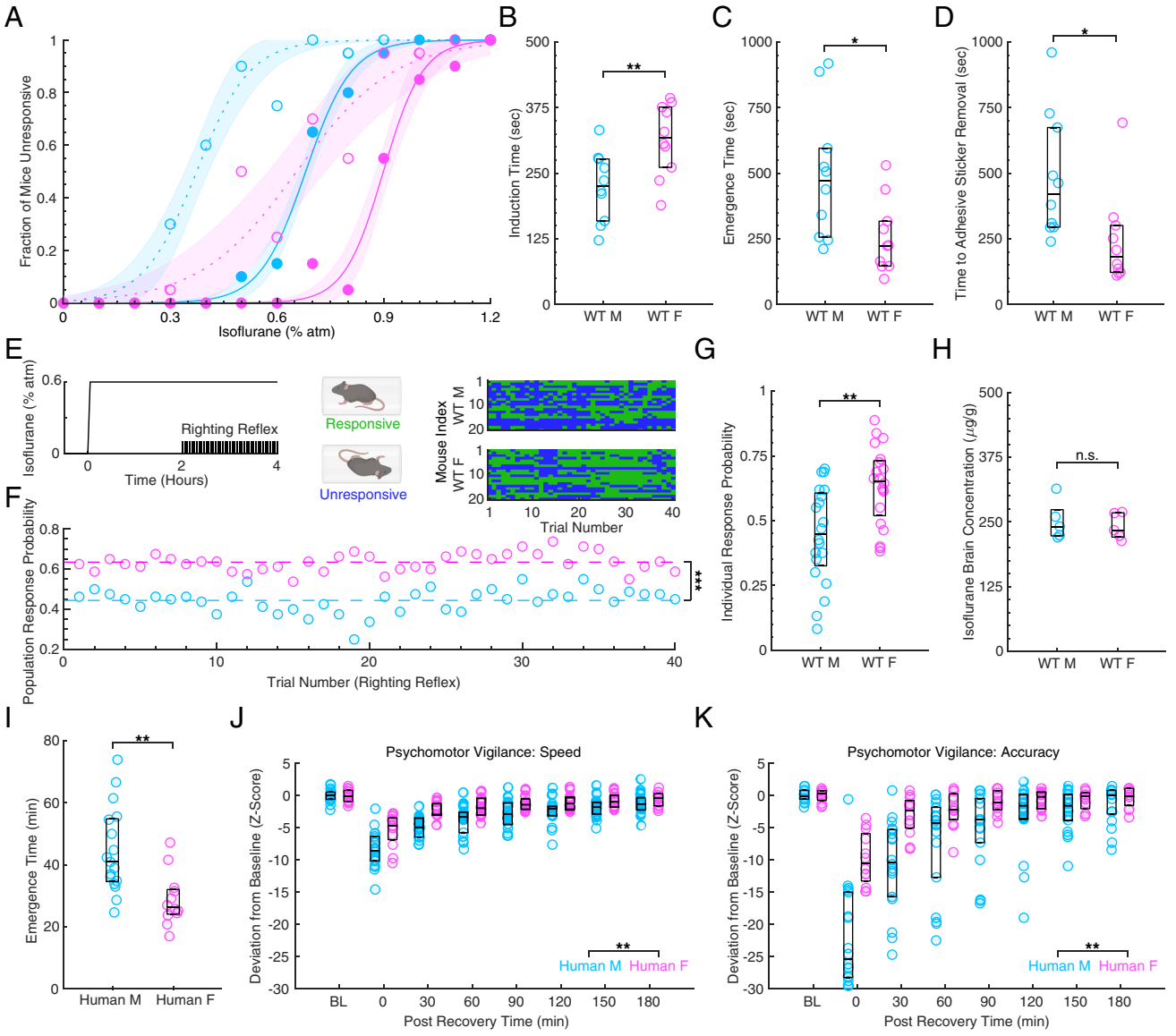

Fig. 1. Behavioral and cognitive measures reveal that females are more resistant to hypnotic effects of isoflurane than males. In all panels, pink denotes females and blue denotes males. (*A*) Righting reflex dose–response for induction (solid dots) and emergence (open dots) for WT M (n = 20) and WT F (n = 20). Solid and dashed lines colored by sex show best-fit sigmoidal curves for induction and emergence, respectively. Shaded regions show 95% CI. (*B*) Time to loss of the righting reflex in WT M (n = 10) and WT F (n = 10) mice exposed to 1.2% isoflurane. (*C*) Time to regain the righting reflex following a 2-h 1.2% isoflurane exposure in WT M (n = 10) and WT F (n = 10) mice. (*D*) Time to remove adhesive sticker attached to snout following a 2-h 1.2% isoflurane exposure in WT M (n = 10) and WT F (n = 10) mice. (*E*) WT M (n = 20) and WT F (n = 20) mice were exposed to 0.6% isoflurane for 4 h. Times at which righting reflex assessments were performed are shown by ticks (green denotes responsive; blue denotes unresponsive for each mouse on every trial). (*F*) Response probability averaged across individuals in WT M and WT F mice as a function of trial number. (*G*) Response probability averaged across trials for each individual WT M and WT F mouse. (*H*) Isoflurane brain concentration in WT M (n = 5) and WT F (n = 5) mice as measured by HPLC after 2 h of isoflurane exposure. (*I*) Emergence times in human volunteers (n = 18 M, n = 12 F) after discontinuation of 3 h of 1.3 age-adjusted MAC of isoflurane. Performance speed (*J*) and accuracy (*K*) on the psychomotor vigilance test in human males and females. Boxes show interquartile ranges and medians. Statistical significance is denoted by **P* < 0.05, ***P* < 0.01, and ****P* < 0.0001. Cartoon schematic in Fig. 1*E* were generated using Biorender.

ANOVA, Sex by Time) on the psychomotor vigilance test upon recovery from anesthesia than males. Altogether, these results offer compelling evidence of increased anesthetic resistance in females as reflected in multiple behavioral and cognitive measures in both mice and humans.

Sex Hormones Modulate Anesthetic Sensitivity. To better understand the genesis of sex differences, we investigated the role of sex hormones on anesthetic sensitivity. We tested postpubertal castrated male (Ca.M) and ovariectomized female (Ov.F) mice and compared their anesthetic sensitivity to gonadally intact controls. Castration resulted in a significant right shift in the induction dose–response curve (Fig. 2*A*) (EC_{50} in Ca.M 0.90% atm., 95% CI [0.88 to 0.92]; WT M (0.68% atm., 95% CI [0.66 to 0.70]) and eliminated all sex differences in anesthetic sensitivity between males and females (EC_{50} in F 0.90% atm., 95% CI [0.88 to 0.92]). In contrast, oophorectomy had no effect on anesthetic sensitivity (EC_{50} in Ov.F 0.91% atm., 95% CI [0.89 to 0.91]). Similar results were observed in the emergence dose–response (*SI Appendix*, Table S2). In our steady-state anesthetic paradigm, (53, 54) castration again produced a female-like anesthetic sensitivity, while ovariectomy again failed to change anesthetic sensitivity. The mean individual righting probability during steady-state 0.6% isoflurane exposures in WT M (0.44 ± 0.19 (mean ± SD) (0.45 [0.31 to 0.61] (median [IQR])) was significantly lower than in Ca.M (0.72 ± 0.20 (0.75 [0.55 to

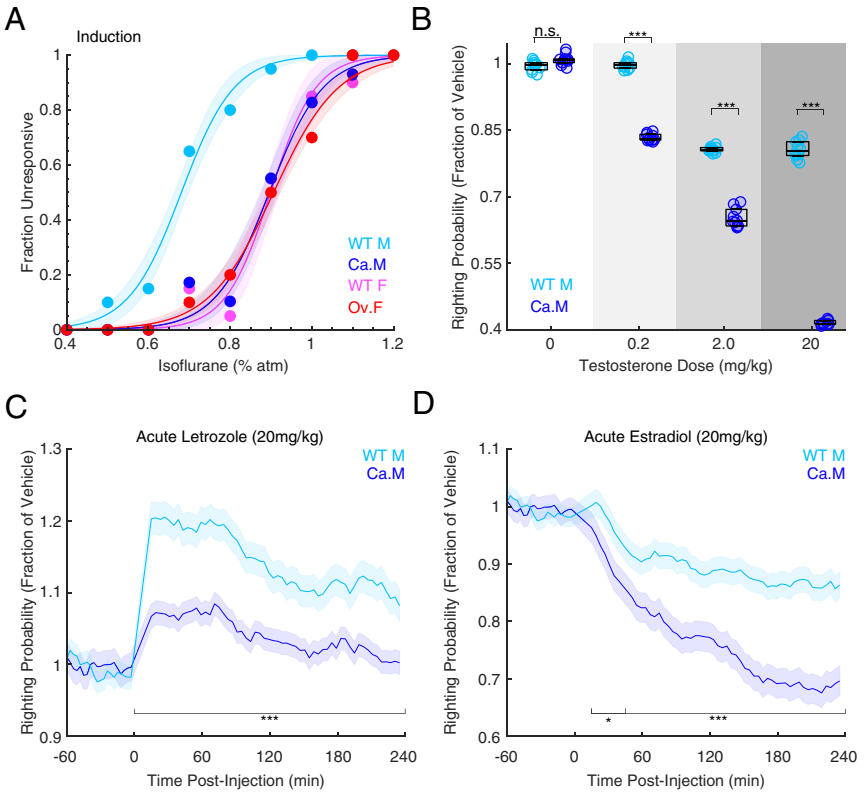

Fig. 2. Sex hormones modulate anesthetic sensitivity. In all panels, pink denotes intact females and blue denotes males. Red and dark blue denote oophorectomized females (Ov. F) and Ca. M, respectively. (*A*) Righting reflex dose–response curves (n = 29 Ca.M, n = 10 Ov.F) and 95% CIs (shading) as in Fig. 1. WT M and WT F data are replotted from Fig. 1 for comparison. (*B*) Effects of acute testosterone administration on anesthetic sensitivity (n = 10 WT M, n = 10 Ca. M). All results are shown as fraction of baseline righting reflex probability measured prior to testosterone administration. The effect was averaged across trials obtained between hours 3 and 4 following testosterone administration. The effect of vehicle (DMSO + corn oil) computed in the same fashion is shown as 0 mg/kg testosterone. (*C*) Effects of acute letrozole administration on righting reflex probability as a function of time. The effect (mean ± SD) is shown as a fraction of baseline righting probability. The probability is averaged across individuals at each trial (n = 10 WT M, n = 10 Ca. M). (*D*) Same as in *C* but for estradiol administration. Multiple comparisons showing significant differences between groups are shown. Boxes show interquartile ranges and medians. Statistical significance is denoted by **P* < 0.05 and ****P* < 0.0001.

0.90])), WT F (0.64 ± 0.15 (0.65 [0.50 to 0.73])), and Ov.F (0.77 ± 0.15 (0.76 [0.66 to 0.93])) ($F_{(3,56)}$ = 10.60, P < 0.0001, 1-way ANOVA, Šídák's multiple comparisons test: WT M vs Ca.M P = 0.0007, WT M vs. WT F P = 0.0054, WT M vs. Ov.F P < 0.0001, Ca.M vs. WT F P = 0.74, Ca.M vs. Ov.F P = 0.99, WT F vs. Ov.F P = 0.25). As before, pharmacokinetic differences were excluded as a hypothetical explanation as no differences in mean brain isoflurane concentrations were detected across the four groups (WT M 251.8 ± 38.2 μg-iso/g-brain tissue (mean ± SD) (241 [222 to 287] (median [IQR]), Ca.M 265.8 ± 41.8 (251.5 [232.3 to 300.3]), WT F 241.2 ± 25.6 (234 [218 to 268]), Ov.F 254.7 ± 40.6 (236 [229 to 282]), $F_{(3,25)}$ = 0.48, P = 0.70, 1-way ANOVA). These results suggest that sex differences in anesthetic sensitivity are primarily due to the presence of testosterone.

To demonstrate the effect of testosterone directly, we studied acute effects of testosterone on anesthetic sensitivity during a steady-state righting reflex experiment in WT M and Ca.M mice. After 2 h of equilibration with 0.6% atm isoflurane, the righting reflex was tested every 3 min for 1 h to establish baseline response probability. Mice were then injected with varying doses of testosterone or vehicle and had their righting reflex assessed for another 4 h. Vehicle injection did not change the mean population response probability across trials in WT M (P = 0.31, unpaired t test) or Ca.M (P = 0.69, unpaired t test) as compared to baseline in each group. However, testosterone administration enhanced anesthetic sensitivity ($F_{(3,72)}$ = 815.9, P < 0.0001, 2-way ANOVA, Gonadal Status by Testosterone Dose) in both intact and Ca.M mice in a dose-dependent fashion (Fig. 2*B*). Durable effects following a single dose of testosterone were not observed during follow-up examination of anesthetic sensitivity 72 h post initial administration ($F_{(1,38)}$ = 0.7950, P = 0.38, repeated measures 2-way ANOVA, Gonadal Status × Baseline Responsiveness over Time). While both WT M and Ca.M became more deeply anesthetized following acute testosterone administration, this effect was significantly greater in castrated animals.

The effects of testosterone on anesthetic sensitivity were apparent within 1 h of subcutaneous administration (*SI Appendix*, Fig. S1; WT M $T_{1/2}$ = 88 min, 95% CI [76 to 104], Ca.M $T_{1/2}$ = 77 min, 95% CI [68 to 88]). This rapid onset of action suggests that the effects of testosterone are unlikely to be mediated by changes in gene expression (58, 59). In addition to the direct androgen receptor–dependent gene expression pathway, testosterone exerts effects on the brain via its conversion to estradiol by aromatase (60). Aromatase expression in the preoptic hypothalamus—an area involved in control of sleep and wakefulness–is sexually dimorphic (61–65). In addition to the effects on gene expression, estradiol exerts a multitude of effects via non-canonical fast pathways that manifest on the time scale of minutes (66). Thus, we hypothesized that testosterone acutely lowers anesthetic sensitivity via its conversion to estradiol by aromatase. To determine whether conversion of testosterone to estradiol contributes to the effects of testosterone on anesthetic sensitivity in males, we administered the aromatase inhibitor, letrozole, to WT M and Ca.M (Fig. 2*C*). Consistent with a role of testosterone's conversion to estradiol in increasing anesthetic sensitivity, inhibition of aromatase reduced anesthetic sensitivity. As expected from the fact

that endogenous levels of testosterone are greatly attenuated after castration, the effect of aromatase inhibition was more pronounced in gonadally intact male mice ($F_{(75,1368)} = 36.51$, $P < 0.0001$, 2-way ANOVA, Gonadal Status by Time).

If testosterone exerts its effects in part through conversion to estradiol, then estradiol should also affect anesthetic sensitivity. This was indeed the case (Fig. 2*D*). Both WT M and Ca.M became acutely more sensitive to isoflurane following estradiol administration ($F_{(75,1368)} = 48.11$, $P < 0.0001$, 2-way ANOVA, Gonadal Status by Time). Cumulatively, these results suggest that testosterone acutely increases anesthetic sensitivity through its conversion to estradiol by aromatase.

Electroencephalographic Measures Do Not Reflect Sex Differences in Anesthetic Sensitivity. Electroencephalographic (EEG) and electrocorticographic (ECoG) features of general anesthesia have been studied and used to quantify anesthetic depth (67, 68). The increasing prevalence of delta oscillations (1 to 4 Hz) is associated with the deepening of the anesthetic state (69, 70). Deep general anesthesia is associated with burst suppression characterized by transient bursts of EEG activity in otherwise isoelectric background (67). We therefore hypothesized that behavioral differences in anesthetic sensitivity would be associated with EEG differences between the sexes. To test this hypothesis, we performed spectral analysis on EEG of WT F and WT M mice exposed to steady-state 0.6% isoflurane. Surprisingly, we were unable to detect sex differences in any frequency bands ($F_{(1,16)} = 0.14$, $P = 0.72$, 2-way ANOVA, Sex by Frequency Band, frontal lead, AP 2.30 mm) (Fig. 3*A*). No sex differences in EEG power were found anywhere along the cortical rostral–caudal axis (AP 1.00 mm, $F_{(1,16)} = 0.47$, $P = 0.50$; AP −0.30 mm, $F_{(1,16)} = 3.27$, $P = 0.089$; AP −1.60 mm, $F_{(1,16)} = 0.00$, $P > 0.99$; AP −2.90 mm, $F_{(1,16)} = 0.082$, $P = 0.78$, 2-way ANOVAs, Sex by Frequency Band). We were also unable to detect differences in the propensity of female and male brains to enter deeper states of anesthesia as determined by the burst suppression ratio (SR) of ECoG under 0.6% isoflurane (WT M 0.025 ± 0.04 (mean ± SD) (0.003 [0 to 0.34] (median [IQR])), WT F 0.006 ± 0.008 (mean ± SD) (0.0004 [0 to 0.014]), U = 105.5, $P = 0.26$, Mann-Whitney *U* test) (Fig. 3*B*) or 1.2% isoflurane (WT M 0.18 ± .13 (mean ± SD) (0.17 [0.05 to 0.29] (median [IQR]), WT F 0.22 ± 0.16 (0.23 [0.09 to 0.31]), $P = 0.45$, unpaired *t* test) (Fig. 3*C*). To determine whether sex differences exist in humans under precisely controlled anesthetic exposures devoid of surgical confounds, we reanalyzed data collected from the ReCCognition trial (49). At 1.3 age-adjusted MAC of steady-state isoflurane, the human EEG was dominated by burst suppression (56). We looked at 3 characteristics of burst suppression: percent time spent in suppression, longest suppression length, and the number of transitions between burst and suppression epochs (56). As in mice, no sex differences were observed in humans (Fig. 3*D*) in any burst suppression measure ($F_{(1,25)} = 1.17$, $P = 0.29$, 2-way ANOVA, Sex by Burst Suppression Metric). Moreover, no correlations between measured EEG metrics and emergence times were observed (*SI Appendix*, Table S3). Cumulatively, these results show that, while sex exerts clear behavioral differences in anesthetic sensitivity in both mice and humans, conventional EEG measures of anesthetic depth do not reveal sex differences in either species.

Whole Brain c-Fos Mapping Reveals Hypothalamic Sex Differences under Anesthesia. While the EEG is capable of distinguishing between the activity in the awake and the anesthetized brain, it may not faithfully reflect subcortical differences in anesthetic sensitivity. We therefore conducted a whole brain screen for the immediate early gene product, c-Fos, whose expression has been used to map antecedent neuronal activity (71). Brains of female and male mice were harvested immediately after 4-h exposure to 0.6% isoflurane, optically cleared, and stained with a c-Fos antibody (72–74). Cleared brains were imaged on a light sheet microscope with sufficient resolution to localize individual c-Fos

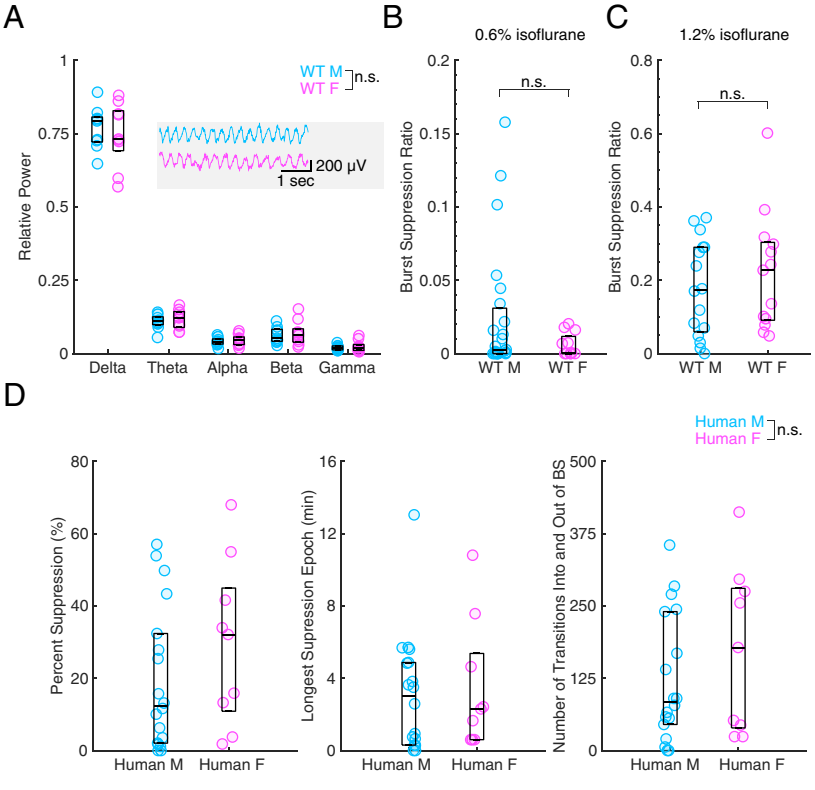

Fig. 3. EEG and ECoG do not reflect sex differences in anesthetic sensitivity. (*A*) Frontal EEG power in the canonical frequency bands in WT M (n = 9) and WT F (n = 9) mice during 0.6% isoflurane exposure. *Inset* shows 5 s traces of raw EEG. (*B*) Burst SRs at 0.6% isoflurane recorded with ECoG over V1 (n = 12 WT F and 23 WT M). (*C*) Same as in *B* but at 1.2% isoflurane (n = 13 WT F and 16 WT M). (*D*) Time spent in suppression, maximum suppression length, and the number of transitions between burst and suppression epochs in human volunteers during 1.3 age-adjusted MAC isoflurane (n = 9 F and 18 M).

immunoreactive neurons across the entire brain. After automated detection and registration (75, 76) to the Allen reference atlas (77), the number of c-Fos-positive neurons in male and female brains were compared in 314 summary structures (77).

To determine whether there were sex differences in c-Fos-positive neuron densities in any summary structures, we computed Bonferroni corrected *t-statistics*. *T-statistics* for each summary structure were computed with the assumption of equal variances ($F_{(313,313)} = 1.22$, $P = 0.082$, F test). This analysis revealed 24 brain structures with significantly different expression of c-Fos under isoflurane as a function of sex (*SI Appendix*, Table S4). To determine whether brain structures with different c-Fos expression in males and females were uniformly dispersed across the brain or concentrated in a particular "major division" as described by the Allen Brain Atlas (77), we computed a permutation test on the t-statistic derived *P*-values across all summary structures and compared number of sexually dimorphic structures in each major division compared to shuffled surrogate data. The hypothalamus was the only major division found to be differentially active under steady-state isoflurane in males and females ($P = 0.0059$, permutation test) (*SI Appendix*, Table S5). Sexually dimorphic hypothalamic structures are located throughout the greater preoptic area (15, 16, 78), which is also known to modulate arousal both during natural sleep (79, 80) and anesthetic-induced unconsciousness (Fig. 4) (2, 11, 81). Compared to females, areas with significantly greater c-Fos expression levels in males included the ventrolateral preoptic, retrochiasmatic area (partially overlapping with the supraoptic nucleus), median preoptic (including the vascular organ of the lamina terminalis), medial preoptic, lateral preoptic, and paraventricular hypothalamic nuclei (for a full list, see *SI Appendix*, Table S4). Activation of all these regions as commonly measured by the nuclear induction of c-Fos is known to potentiate sleep and/or promotes anesthetic hypnosis (7–10, 82–85). We similarly performed whole-brain c-Fos activity mapping in Ca.M and compared to intact WT M counterparts. Brain regions exhibiting differential c-Fos activity patterns in castrated compared to gonadally intact males resembled the differences between WT M and WT F (*SI Appendix*, Fig. S2). Notably, ventral hypothalamic structures were enriched with c-Fos expression in the more sensitive WT M (*SI Appendix*, Table S6). Collectively, these results suggest that sexually dimorphic activity patterns of hypothalamic sleep-promoting structures consistently correlate with anesthetic sensitivity.

Discussion

Here, we directly demonstrate that the female brain is more resistant to the hypnotic effects of volatile anesthetics. Sex differences in anesthetic sensitivity are predominantly due to testosterone. Testosterone acutely increases anesthetic sensitivity through an aromatase-dependent conversion to estradiol. Finally, we demonstrate that sex differences in anesthetic sensitivity are conserved between mice and humans.

The existence of sex differences in anesthetic sensitivity has been suggested by some previous clinical (23, 37) and animal studies (43, 44, 46). However, a major limitation of the previous work was that the sex differences in anesthetic sensitivity were confounded by differences in drug absorption and elimination. While it is possible that pharmacokinetic differences exist between males and females, here we demonstrate that such differences cannot account for the observed differences in anesthetic sensitivity. To accomplish this, we utilized a behavioral paradigm developed in our lab (53, 54), which allows us to study behavioral responses under steady-state anesthetic administration (55). To further support the conclusion that differences in anesthetic sensitivity cannot be solely due to differences in drug absorption, we directly confirmed that the steady-state concentration of isoflurane in the brain does not depend on sex or hormonal milieu.

Accumulating evidence across mechanistically distinct anesthetics, model organisms, and experimental techniques points to the importance of hypothalamic nuclei involved in the control of sleep and wakefulness in mediating the hypnotic effects of anesthetics (4, 7–9, 44, 82, 83, 86–88). Interestingly, the same hypothalamic nuclei are some of the most sexually dimorphic brain structures (89, 90). This observation led to the hypothesis that the responses of the male and the female brain to anesthetics ought to differ. Our behavioral analyses in both mice and humans are consistent with this hypothesis. An unbiased whole brain c-Fos screen revealed more active neurons in the ventral hypothalamic nuclei of the male brain. Castration increases anesthetic resistance and concomitantly decreases the number of active neurons in the sleep- and anesthesia-promoting regions of the ventral hypothalamus. Altogether, these results argue that the sex differences in anesthetic sensitivity may be due to the differential effects of anesthetics on the male and female hypothalamic nuclei.

The testosterone-induced increase in anesthetic sensitivity is readily observable minutes after subcutaneous administration. This rapid onset makes it unlikely that the effects of testosterone depend on the canonical signaling pathway. Canonical signaling pathways for sex hormones involve changes in gene expression that unfold over the course of hours to days. Sex hormones also produce rapid effects on neuronal activity through non-canonical pathways (91). The specific molecular mechanisms through which testosterone and estradiol increase anesthetic sensitivity are beyond the scope of this work. It is worth noting, however, that steroid compounds can be used to rapidly induce anesthesia (92). The hypnotic effects of neurosteroids depend strongly on their interactions with $GABA_A$ receptors (93–95). The actions of neurosteroids on $GABA_A$ receptors are sexually dimorphic (96, 97). It is therefore possible that the direct actions of sex hormones on the $GABA_A$ receptor contribute to their effects on anesthetic sensitivity. This hypothesis can be addressed in future work.

Since the 1930s, the hypnotic effects of anesthetics have been quantified using the EEG (98). To this day, most commonly used modes of assessing anesthetic depth rely on the EEG signals (68). Interestingly, while multiple behavioral measures in mice and in humans converge on the fact that females are more resistant to anesthetics than males, the EEG or ECoG recorded under steady-state anesthesia does not exhibit sex differences at either intermediate or high anesthetic concentrations. Across the cortex, anesthetic active neurons are similarly distributed in males and females. Previous work (44) observed some sex differences in the EEG of mice exposed to sevoflurane. These experiments were not performed under steady-state conditions and consequently could not exclude a potential pharmacokinetic confound. We did not evaluate sex differences in the EEG under sevoflurane, so it remains possible that the discrepancy between our results and those in ref. 44 are due to the differences in anesthetic agent. Thus, while our analysis cannot exclude small sex differences in cortical activity observable at the level of individual neurons, the confluence of evidence suggests that the primary locus responsible for the sex differences in anesthetic sensitivity lies outside the cortex.

One limitation of our study is its reliance on c-Fos staining as a marker of neuronal activity. It is presently unclear whether sex differences in c-Fos expression point to the existence of distinct neuronal subtypes active under anesthesia. While we show a correlation between anesthetic sensitivity and c-Fos expression in the hypothalamus, neuronal activity would have to be exogenously manipulated to obtain causal evidence. Present methods for such manipulations

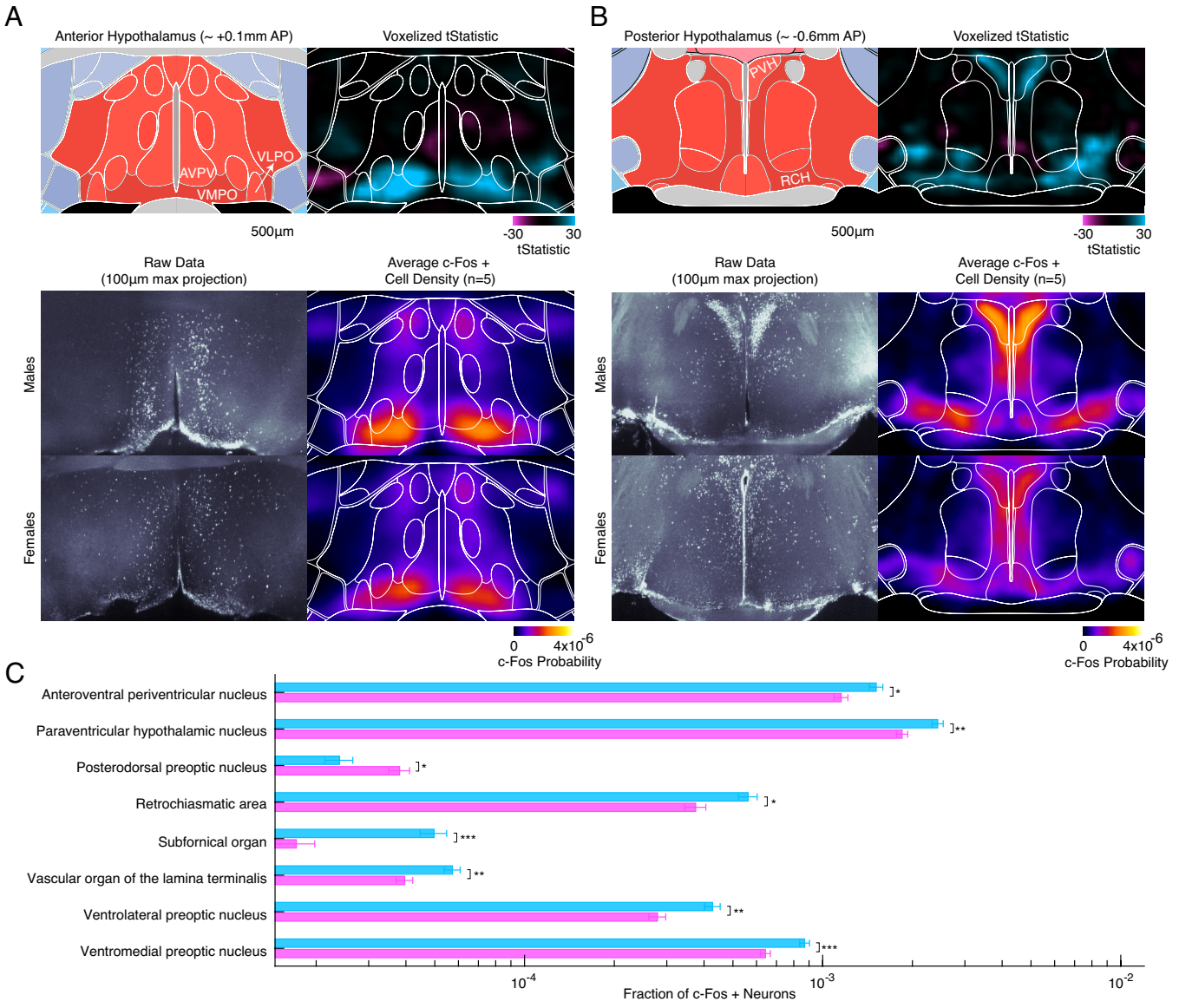

Fig. 4. There are fewer c-Fos-positive neurons in sleep-promoting hypothalamic nuclei of anesthetized female mice. (*A*) Anterior and (*B*) posterior hypothalamic coronal representations from Allen mouse brain reference annotation atlas (*Upper Left*), voxelized t-statistic map displaying differences in c-Fos immunoreactivity as a function of sex (*Upper Right*), coronal images of raw c-Fos expression (*Middle* and *Lower Left*), and average c-Fos nuclear density maps (*Middle* and *Lower Right*) in male and female mice following a 4-h 0.6% isoflurane exposure (n = 5 WT M and 5 WT F). For the t-statistic maps, blue depicts regions with higher c-Fos density in males, whereas pink depicts regions with higher c-Fos density in females. (*C*) After correction for 314 discrete Allen Brain Atlas summary structures, c-Fos cell densities in 8 hypothalamus sites differed significantly between WT F and WT M. Bar graphs show mean ± SD. Allen mouse brain reference annotation atlas abbreviations are as follows—AVPV: anteroventral periventricular nucleus, VMPO: ventromedial preoptic nucleus, VLPO: ventrolateral preoptic nucleus, PVH: paraventricular hypothalamic nucleus, RCH: retrochiasmatic area. Statistical significance is denoted by $^{*}P < 0.05$, $^{**}P < 0.01$, and $^{***}P < 0.0001$.

remain rather coarse. Without a more detailed understanding of the distinct molecular subtypes of hypothalamic neurons activated by anesthetics and their activity patterns in males and females, such manipulations are unlikely to yield meaningful results. While we clearly show acute effects of sex hormones on anesthetic sensitivity, it is possible that, in addition to these acute effects, sex hormones may also produce long-lasting effects on anesthetic sensitivity. This possibility should be addressed in future work.

In clinical settings, anesthetic administration is typically guided by data disproportionally compiled in males. As we demonstrate, this approach may significantly underestimate anesthetic requirements for female patients. Alternatively, anesthetics can be titrated to specific EEG end points. However, EEG does not always faithfully reflect the state of consciousness. Behavioral and EEG-based assessment of anesthetic depth can be discordant (51, 99–101). Conventional methods for estimating anesthetic depth do not reliably detect episodes of awareness under anesthesia (102–109). Collectively, our results add to this evidence by showing that significant sex differences in anesthetic sensitivity are not readily detectable in the EEG. This discordance between behavioral and encephalographic measures of the anesthetized state may explain the higher incidence of intraoperative awareness in female patients.

Materials and Methods

Animals. Studies were approved by the Institutional Animal Care and Use Committee at the University of Pennsylvania and were conducted in accordance with the NIH guidelines. Intact WT M and female (WT F) C57BL/6J mice aged 10 to 30 wk were used throughout this study (Stock No. 000664, Jackson Laboratories, ME). Castrated (Ca.M) and ovariectomized (Ov.F) C57BL/6j mice were obtained from Jackson laboratories (Stock No. 000664, Jax Surgical Services, Jackson Laboratories, ME). Gonadectomies were performed on adult mice at least 3 wk

prior to any experimental testing. Mice were housed on a 12 h:12 h light–dark cycle (ZT0/lights on at 6:00pm) with ad libitum access to food and water.

For behavioral experiments, mice were habituated to gastight, temperature-controlled, 200 mL cylindrical chambers with 100% oxygen flowing at 200 mL/min for 2 h per day for 3 d prior to experimentation, as previously described (110). Mice were given a minimum of 72-h recovery between anesthetic sensitivity testing assessments. Anesthetic concentrations were confirmed using a Riken FI-21 refractometer (AM Bickford). All subsequent behavioral procedures followed this outlined procedure unless otherwise noted. For all anesthetic exposure experiments, mice were kept normothermic by placing all righting reflex cylinders in a 37 °C water bath (110).

Drug Preparations. Vehicle for drug administration consisted of dimethyl sulfoxide (DMSO) and corn oil (1:9, v/v). Testosterone (Sigma–Aldrich T1500) doses used throughout the study were 0.2, 2.0, and 20 mg/kg. Letrozole (Sigma Aldrich L6545) and estradiol (Sigma Aldrich E8875) dosing used throughout the study was 20 mg/kg. Drug injections for hormonal studies were performed subcutaneously with freshly made solutions for all experiments.

Dose–Response. Mice were exposed to increasing, then decreasing concentrations of isoflurane, from 0.00 to 1.20% back to 0.00% in 0.20% increments (n = 20 WT M, 20 WT F, 29 Ca.M, 10 Ov.F). Data acquired from two experimental sessions ("even" and "odd" doses) were then combined to have a dose–response curve at a 0.10% step resolution (86). Separate cohorts of mice were exposed to sevoflurane (n = 10 WT M, 10 WT F) from 0.60 to 2.40% in 0.20% step resolution, halothane (n = 10 WT M, 10 WT F) from 0.00 to 1.00% at a 0.10% step resolution, and desflurane (n = 10 WT M, 10 WT F) from 1.50 to 6.00% at a 0.50% step resolution. Mice were exposed to each concentration step for 15 min prior to righting reflex assessment. Flow rates of one volume turnover per minute have been shown to equilibrate chambers within 5 min (53) with resulting brain concentrations equilibrating in approximately 10 min (55). An animal was considered to have an intact righting reflex if it was able to return to a prone position when rotated on its back, otherwise the righting reflex was considered absent. A two-parameter Hill equation was used to fit the mean responses of the induction and emergence arms,

$$1 - R = \frac{1}{1 + e^{H*([Drug] - EC_{50})}},$$

where R is the righting probability, [*Drug*] is the drug concentration, and the two parameters H and EC_{50} are the Hill slope and half maximal effect concentration. EC_{50} and Hill slope estimates and 95% CIs were computed in Matlab with the *nlinfit, nlparci, and nlpredci* functions respectively using the Jacobian of the nonlinear regression model (86).

Induction and Emergence Times. Mice (n = 10 WT M, 10 WT F) were exposed to 1.20% isoflurane in 100% oxygen, where time to loss of the righting reflex was measured. Mice were continuously rotated to a supine position until they were unable to reorient themselves to a prone position. Time to loss of righting was measured, starting from onset of anesthetic delivery. After loss of the righting reflex was achieved, rotation of the chamber stopped, and mice were continuously exposed to 1.20% isoflurane for a total of 2 h from the start of isoflurane delivery. To measure emergence time, mice were rotated into a supine position, isoflurane delivery stopped, and time to spontaneous return of the righting reflex was recorded, as measured by the animal's ability to spontaneously return to a prone position.

Adhesive Sticker Removal Test. Prior to anesthetic exposure, WT M and WT F mice (n = 10 WT M, 10 WT F) were trained for 3 d for sticker removal. While hand restrained, a 0.25-inch diameter round sticker was placed firmly on the animal's snout. Mice were released from the hand restraint and placed into a clean and empty mouse housing cage, where time to removal of the adhesive from the snout was measured. Mice were considered trained when they were able to remove the sticker from their snout in less than 10 s on two consecutive assessments (50).

Trained mice were exposed to 1.20% isoflurane for 2 h. Mice were removed from the chamber, and adhesive sticker was placed immediately upon the snout. Time to removal of the sticker was measured from the time the mouse was removed from the anesthetic chamber to when the sticker was removed from the snout. A sticker removal test was performed on three separate occasions and mean time to sticker removal was used for analysis.

Repeated Righting Reflex Assessment at Steady-State Anesthetic Exposure. For steady-state anesthetic sensitivity testing, habituated mice were exposed to 0.60% isoflurane for 4 h on four separate occasions, as previously described (53, 54). The righting reflex was assessed every 3 min during the final 2 h of a 4-h exposure (n = 20 WT M, 20 WT F, 10 Ca.M, 10 Ov.F). Population response probabilities were computed by averaging the population response probabilities for each righting reflex trial across experimental days. Individual response probabilities were computed by calculating the mean righting probability for each animal across experimental days.

For studies examining the effect of acute hormone administration on steady-state anesthetic sensitivity, mice (n = 10 WT M, 10 Ca.M) were exposed to 0.60% isoflurane while having their righting reflex assessed every 3 min for in the last hour of a 3-h anesthetic exposure prior to receiving an IP injection of vehicle, testosterone, letrozole, or estradiol. Mice were briefly removed from experimental chambers, injected with drug or vehicle, and immediately reinserted into the chambers. Time exposed to open air during the injection time was less than 20 s per mouse. After a 15-min re-equilibration period, mice were subjected to an additional 4 h of righting reflex assessments at 3-min intervals. Animals were exposed twice, and mean population righting probabilities post drug injection were analyzed.

To estimate the kinetics of acute administration of testosterone, the post testosterone population response data were fit to a single exponential: $P(t) = P_0 e^{-kt}$, where $P(t)$ is the population response probability at time t after injection, and P_0 and k are the initial response probability before testosterone administration and time constant, respectively. Best fit and confidence bounds were estimated using the *fit* and *confint* functions implemented in Matlab. Half-life was then computed as ln(2)/k.

To determine the drug effect compared to vehicle control, mean population-level responses from each group were computed as a change in anesthetic sensitivity from vehicle responsiveness. Error estimation was computed with a moving window computing both mean and SD in anesthetic sensitivity across trials (20 trial window size, 1 trial step size).

Whole-Brain Isoflurane Concentration Quantification. Mice (n = 5 WT M, 5 WT F, 10 Ca.M, 9 Ov.F) were exposed to 1.00% isoflurane for 2 h and then rapidly killed by cervical dislocation to quantify whole brain isoflurane concentrations. Brains were subjected to high-performance liquid chromatography analysis as previously described (55, 87).

EEG Implantation, Recording, and Analysis. Mice (n = 9 WT M, 9 WT F) were induced with 2.50% isoflurane in 100% oxygen and maintained at 1.50% isoflurane for the duration of the EEG implantation surgery. After a surgical plane of anesthesia was reached, as measured by the lack of a toe pinch response, mice were placed in a stereotactic frame (Kopf Model 940). Core body temperature was maintained with a closed-loop heating pad (TC1000, CWE Inc), and the eyes were protected with eye ointment. Electrodes were constructed and implanted as previously described (111). Nine epidural EEG leads were implanted 0.65 mm lateral to bregma in both hemispheres, ranging from 2.30 mm anterior to bregma to −2.90 mm posterior to bregma. Headpieces were secured using dental cement (A-M Systems) and two anchor screws (McMaster-Carr 91800A050), positioned at 2.50 mm lateral and 2.00 mm posterior to Bregma. Mice were allowed to recover from the implant for a minimum of 1 wk prior to experimentation. Upon recovery, mice were habituated to cable tether within the experimental recording chamber over three 2-h sessions. During recording, mice were exposed to 0.6% isoflurane in 100% oxygen for 60 min. Core temperature was maintained with a water bath (55). The final 30 min of recording were used for subsequent analysis.

EEG signals were recorded at 1 kHz with 32 channel headstages (C3324, Intan Technologies, Los Angeles, CA) as previously described (111, 112). EEG signals were low passed with a 6th-order, zero-phase Butterworth filter at a cutoff frequency of 50Hz. Multitaper spectral estimation was used to compute spectrograms under experimental conditions (15 tapers, 60-s non-overlapping windows normalized to total power per window) (113). For each animal, mean power across windows was compared across groups to determine if there were differences in spectral power under steady-state isoflurane administration. Canonical bins of

delta (<4 Hz), theta (4 to 8 Hz), alpha (8 to 12 Hz), beta (12 to 30 Hz), and gamma (>30 Hz) were utilized for analysis (Fig. 3*A*).

Local Field Potential Recordings and Burst Suppression Identification. Local field potential (LFP) data examined throughout this study were collected as a part of previous studies from refs. 106 and 107 where the study design has been previously described in detail. Briefly, anesthetized mice were placed in a stereotaxic frame and a craniotomy was drilled from 1.00 mm to 5.00 mm AP and 6.00 mm to 0.25 mm ML. A 64-electrode surface grid (Neuronexus E64-500-20-60) was positioned over the dura to obtain ECoG signal. Mineral oil was applied on top of the ECoG grid every 20 min to preserve the health of the underlying dura and brain. Mice were exposed to 0.6% (n = 23 WT M, 16 WT F) and 1.2% (n = 16 WT M, 13 WT F) isoflurane and unstimulated LFP was recorded. Animals were scarified the same day immediately after the final recording session.

ECoG signals were recorded at 30 kHz with headstage (Neuralynx HS36) digitized through the Cheetah 64 acquisition system (Neuralynx ERP-27 Lynx-8). Signals were bandpassed between 0.1 Hz and 325 Hz with a zero-phase custom-built FIR filter. Signals were then decimated to 1 kHz and mean re-referenced after manual channel artifact rejection. Multitaper spectral estimation was used to compute spectrograms for each isoflurane concentration (20 tapers, normalized to total power per window). Unstimulated LFP was used for spectral analysis. Of note, 95% CIs were estimated from the ensuing normalized power spectra.

Both a frequency and amplitude metric was used to determine periods of suppression in the LFP recordings as previously described (114). Total power of preprocessed signal windows from 2 to 100 Hz were subjected to k-means clustering for 2 clusters, where clusters correspond to suppressed or non-suppressed windows. A maximal amplitude threshold of the total power feature was then manually selected for each animal. Concurrently, RMS was also calculated over the LFP data in 500-ms windows with 400-ms window overlap. A manual maximum RMS threshold was selected for each mouse. Time windows were classified as suppression if the total power and RMS were below their respective thresholds. The SR was calculated by the number of time windows with suppression divided by the total number of time windows (Fig. 3 *B* and *C*).

Whole Brain Mapping of Neural Activity. Mice exposed to 0.6% isoflurane for 4 h were rapidly killed and transcardially perfused using ice-cold PBS with heparin (10 U/mL) followed by 4% paraformaldehyde. (n = 5 WT M, 5 WT F, 5 Ca.M) Brains were removed and post-fixed in 4% paraformaldehyde at 4 °C overnight. Whole brains were then washed in PBS and shipped to LifeCanvas Technologies (Cambridge, MA) in a PBS with 0.02% sodium azide solution for further processing, staining, imaging, and mapping.

Whole mouse brains were processed following the SHIELD protocol (72) (LifeCanvas Technologies). Samples were cleared for 5 d at 42 °C with SmartClear II Pro (LifeCanvas Technologies), a device employing stochastic electrotransport (73). Cleared samples were then actively immunolabeled using SmartLabel (LifeCanvas Technologies) based on eFLASH technology integrating stochastic electrotransport (73) and SWITCH (74). Each brain sample was stained with primary antibody, 3.5 mg of rabbit anti-c-Fos monoclonal antibody (Abcam, #ab214672) followed by fluorescently conjugated secondary in 3:2 primary:secondary molar ratio (Jackson ImmunoResearch). After active labeling, samples were incubated in EasyIndex (LifeCanvas Technologies) for refractive index matching (RI = 1.52) and imaged at 3.6× with a SmartSPIM axially swept light sheet microscope (LifeCanvas Technologies).

Sample images were tile corrected, destriped, and registered to the Allen Brain Atlas (Allen Institute: https://portal.brain-map.org/) using an automated process. An autofluorescence channel for each brain was registered to 8 to 20 atlas-aligned reference samples, using successive rigid, affine, and b-spline warping algorithms (SimpleElastix: https://simpleelastix.github.io/). An average alignment to the atlas was generated across all intermediate reference sample alignments to serve as the final atlas alignment value for the sample. Automated cell detection was performed using a custom convolutional neural network through the Tensorflow python package. The cell detection was performed by two networks in sequence. First, a fully convolutional detection network (75) based on a U-Net architecture (75) was used to find possible positive locations. Second, a convolutional network using a ResNet architecture (76) was used to classify each location as positive or negative.

Whole Brain c-Fos Density Estimation and Voxel Registration to Summary Structures. For each brain, c-Fos positive cells were assigned 3D coordinates referenced to the Allen Brain Atlas (77). Individual JSON files can be found online at https://zenodo.org/record/8384835. Assigned coordinates had to be located within the boundaries of the reference atlas brain volume; otherwise they were rejected. Coordinates of all c-Fos positive cells were pooled together for males and for females. Random resampling with replacement (100 bootstrapped samples) was used to estimate the mean and the SD of the number of neurons in each 50 × 50 × 50 μm voxel. The distribution was filtered with a gaussian filter ($\sigma = 1$ voxel). Cell counts in each voxel were normalized by the total cell count across all voxels. The t-statistic maps (Fig. 4) were computed on the voxel basis using estimates of the means and the SD.

Voxels were then assigned to "Summary Structures" as identified by Wang et al. (77) We limited our analysis to regions under the Allen Reference Atlas CCFv4 Ontology core label of "Basic cell groups and regions" and to regions that were nonoverlapping with respect to voxel registration. This left 314 summary structures. Children of summary structures were reassigned from the annotation reference atlas (annotation_50.nrrd from Allen Brain Institute) to match summary structure IDs. To compute a t-statistic between male and female groups at the summary structure level, means and SD of each voxel within a summary structure were summed together. A Bonferroni correction for multiple comparisons was utilized to determine an adjusted alpha for statistical significance ($a_{adj} = 1.59 \times 10^{-4}$).

To determine whether any major brain divisions had a significant proportion of sexually dimorphic structures, we computed a permutation test. Statistical significance of this proportion was assessed using a permutation test (10,000 permutations).

Human Volunteers. Data were collected as a part of the ReCCognition (NCT01911195) study with appropriate institutional review board approval: University of Pennsylvania, Philadelphia, PA (Protocol #818401), University of Michigan, Ann Arbor, MI (Protocol #HUM0071578), and Washington University in St. Louis, St. Louis, MO (Protocol #201308073). This study design has been previously described in detail (49). Study participants were recruited via public flyers and financially compensated for their voluntary participation with ethics committee approval. Study risks and eligibility criteria were discussed in detail and reviewed with all volunteers who provided their written informed consent in accordance with the Declaration of Helsinki. Briefly, 30 healthy, young volunteers (18 men and 12 women, 22 to 40 y old) were administered isoflurane 1.3 age-adjusted MAC for 3 h. EEG was continuously recorded from volunteers throughout the anesthetic exposure. Physiological monitoring was in place to keep volunteers normothermic. At the end of the anesthetic challenge, volunteers were played an auditory cue, repeated every 30 s, asking to squeeze either hand twice. Recovery from anesthesia was defined by being able to correctly respond to the auditory cue on two consecutive assessments. Emergence time was recorded as the time from discontinuation of isoflurane to the time of recovery.

Human Volunteer Neurocognitive Testing. Volunteers went through the Cognition test battery (115) testing every 30 min for 180 min after recovering from anesthesia (57). Here, we focused on the Psychomotor Vigilance Test (PVT), an assay using reaction time to assess cognitive vigilance, awareness, and attention that is immune to a learning effect (116, 117). In order to consider a speed-accuracy tradeoff, both PVT speed and accuracy were analyzed separately (118). PVT recovery assessments were normalized to baseline mean speed or accuracy performance for each sex.

Human Volunteer EEG Burst Suppression Identification. Human EEG data examined throughout this study were collected as a part of ReCCognition study. EEG processing and burst suppression identification for this dataset was described previously by Shortal et al. (56). Briefly, EEG signals were recorded at 500 Hz using the Electrical Geodesics EEG system (Eugene, OR) referenced to Cz. Signals from the F3 lead were high pass filtered at 0.1 Hz using a 4th-order Butterworth filter. Multitaper spectral estimation was used to compute spectrograms (5 tapers, 10-s window length, 1-s window overlap) (113). Spectrograms for each volunteer were subjected to principal component analysis and Hartigan's dip statistic (119) was used to determine whether the first principal component was unimodal or not. If unimodality was rejected, k-means clustering was performed on the first two principal components of the data, resulting in a suppressed and non-suppressed cluster, which classified each spectral window.

Quantification and Statistical Analysis. Data were processed and analyzed in Matlab (2023a, Mathworks, Natick Ma) using the Signal Processing, Image Processing, Curve Fitting, and Statistics and Machine Learning Toolboxes. For dose–response studies, statistical significance was computed based using the 95% CIs of the parameters of best fit model. If the CIs did not overlap, the results were deemed to be significant (120). EEG spectral estimation used computed using custom code written by Hudson et al. (113). Statistical comparisons were performed using Prism 10.0.2 (GraphPad Software, San Diego, CA, USA). Data were tested for normality, using the Shapiro–Wilk test. Appropriate parametric or nonparametric statistical comparison tests were used, and summary statistics are reported within the text. Reported values are both (mean ± SD) and (median [interquartile range (IQR)]) unless otherwise noted. Of note, 95% confidence bounds for fit estimates are reported in the text. For figures, raw data points are shown with overlaid median and IQR for comprehensive visualization of all data. Median and interquartile ranges are reported even for parametric statistical comparisons for figure comparison. In Fig. 4*C*, data are shown as mean ± SD as these are summary structure values generated from bootstrap resampling. $P < 0.05$ was considered statistically significant for all comparisons with appropriate corrections for multiple comparisons.

Data, Materials, and Software Availability. c-Fos Mapping Dataset data have been deposited in Zenodo (https://doi.org/10.5281/zenodo.8384835). All study data are included in the article and/or supporting information. Previously published data were used for this work (Male mouse data from Fig. 1 *F* and *G* was originally published in the following articles: refs. 53 and 54. Mouse EEG data from Fig. 3 *B* and *C* was reanalyzed from the following articles: refs. 114 and 121. Human Data from Fig. 1 *I–K* were reanalyzed from the following article: ref. 57. Human Data from Fig. 3*D* was reanalyzed from the following article: ref. 56.

ACKNOWLEDGMENTS. This work was supported by a collaborative grant from the James S. McDonnell Foundation, St. Louis, MO, and the NIH Grants T32 NS091006 (A.Z.W.), T32 HL007953 (M.E.S.), R01 GM144377 (M.B.K./A.P.), R01 GM088156 (M.B.K.), and R01 GM124023 (A.P.), R01 GM151556 (M.B.K./A.P.). Additional support was provided by the Department of Anesthesiology and Critical Care at the University of Pennsylvania. We would like to thank members of the Center for the Neuroscience of Unconsciousness and Reanimation Research Alliance for their helpful discussions about the data.

Author affiliations: [a]Department of Anesthesiology and Critical Care, University of Pennsylvania, Philadelphia, PA 19104; [b]Neuroscience of Unconsciousness and Reanimation Research Alliance, Department of Anesthesiology and Critical Care, University of Pennsylvania, Philadelphia, PA 19104; [c]Department of Bioengineering, University of Pennsylvania, Philadelphia, PA 19104; [d]Department of Neuroscience, University of Pennsylvania, Philadelphia, PA 19104; [e]Center for Consciousness Science, Department of Anesthesiology, University of Michigan Medical School, Ann Arbor, MI 48105; [f]Department of Anesthesiology, Washington University School of Medicine, St. Louis, MO 63110; and [g]Mahoney Institute for Neurosciences, Perelman School of Medicine, University of Pennsylvania, Philadelphia, PA 19104

1. J. G. Meara *et al.*, Global Surgery 2030: Evidence and solutions for achieving health, welfare, and economic development. *Lancet Lond. Engl.* **386**, 569–624 (2015).
2. N. P. Franks, General anaesthesia: From molecular targets to neuronal pathways of sleep and arousal. *Nat. Rev. Neurosci.* **9**, 370–386 (2008).
3. O. A. Moody *et al.*, The neural circuits underlying general anesthesia and sleep. *Anesth. Analg.* **132**, 1254 (2021).
4. Y. Ma *et al.*, Galanin neurons unite sleep homeostasis and α2-adrenergic sedation. *Curr. Biol.* **29**, 3315–3322.e3 (2019).
5. O. Zalucki, B. van Swinderen, What is unconsciousness in a fly or a worm? A review of general anesthesia in different animal models. *Conscious. Cogn.* **44**, 72–88 (2016).
6. B. Kottler *et al.*, A sleep/wake circuit controls isoflurane sensitivity in Drosophila. *Curr. Biol.* **23**, 594–598 (2013).
7. L.-F. Jiang-Xie *et al.*, A common neuroendocrine substrate for diverse general anesthetics and sleep. *Neuron* **102**, 1053–1065.e4 (2019).
8. J. T. Moore *et al.*, Direct activation of sleep-promoting VLPO neurons by volatile anesthetics contributes to anesthetic hypnosis. *Curr. Biol.* **22**, 2008–2016 (2012).
9. Z. Zhang *et al.*, Neuronal ensembles sufficient for recovery sleep and the sedative actions of α2 adrenergic agonists. *Nat. Neurosci.* **18**, 553–561 (2015).
10. L. E. Nelson *et al.*, The α2-adrenoceptor agonist dexmedetomidine converges on an endogenous sleep-promoting pathway to exert its sedative effects. *Anesthesiol. J. Am. Soc. Anesthesiol.* **98**, 428–436 (2003).
11. S. L. Reitz, M. B. Kelz, Preoptic area modulation of arousal in natural and drug induced unconscious states. *Front. Neurosci.* **15**, 120 (2021).
12. C. B. Saper, T. C. Chou, T. E. Scammell, The sleep switch: Hypothalamic control of sleep and wakefulness. *Trends Neurosci.* **24**, 726–731 (2001).
13. G. Raisman, P. M. Field, Sexual dimorphism in the neuropil of the preoptic area of the rat and its dependence on neonatal androgen. *Brain Res.* **54**, 1–29 (1973).
14. W. T. Greenough, C. S. Carter, C. Steerman, T. J. DeVoogd, Sex differences in dendritic patterns in hamster preoptic area. *Brain Res.* **126**, 63–72 (1977).
15. R. A. Gorski, J. H. Gordon, J. E. Shryne, A. M. Southam, Evidence for a morphological sex difference within the medial preoptic area of the rat brain. *Brain Res.* **148**, 333–346 (1978).
16. R. A. Gorski, R. E. Harlan, C. D. Jacobson, J. E. Shryne, A. M. Southam, Evidence for the existence of a sexually dimorphic nucleus in the preoptic area of the rat. *J. Comp. Neurol.* **193**, 529–539 (1980).
17. L. S. Allen, M. Hines, J. E. Shryne, R. A. Gorski, Two sexually dimorphic cell groups in the human brain. *J. Neurosci.* **9**, 497–506 (1989).
18. M. D. Madeira, N. Sousa, A. Cadete-Leite, A. R. Lieberman, M. M. Paula-Barbosa, The supraoptic nucleus of the adult rat hypothalamus displays marked sexual dimorphism which is dependent on body weight. *Neuroscience* **52**, 497–513 (1993).
19. C. B. Saper, "Chapter 31–The intermediate nucleus in humans: Cytoarchitecture, chemoarchitecture, and relation to sleep, sex, and Alzheimer disease" in *Handbook of Clinical Neurology*, D. F. Swaab, F. Kreier, P. J. Lucassen, A. Salehi, R. M. Buijs, Eds. (Elsevier, 2021), **vol. 179**, pp. 461–469.
20. P. Wang *et al.*, Neural functions of hypothalamic oxytocin and its regulation. *ASN Neuro* **14**, 17590914221100706 (2022).
21. J. M. Schober, D. Pfaff, The neurophysiology of sexual arousal. *Best Pract. Res. Clin. Endocrinol. Metab.* **21**, 445–461 (2007).
22. E. I. Eger, M. J. Laster, G. A. Gregory, T. Katoh, J. M. Sonner, Women appear to have the same minimum alveolar concentration as men: A retrospective study. *Anesthesiology* **99**, 1059–1061 (2003).
23. R. Lennertz *et al.*, Connected consciousness after tracheal intubation in young adults: An international multicentre cohort study. *Br. J. Anaesth.* **130**, e217–e224 (2022), 10.1016/J.BJA.2022.04.010.
24. P. S. Sebel *et al.*, The incidence of awareness during anesthesia: A multicenter United States study. *Anesth. Analg.* **99**, 833–839 (2004).
25. J. J. Pandit *et al.*, 5th National Audit Project (NAP5) on accidental awareness during general anaesthesia: Summary of main findings and risk factors. *Br. J. Anaesth.* **113**, 549–559 (2014).
26. S. O. V. Ranta, R. Laurila, J. Saario, T. Ali-Melkkilä, M. Hynynen, Awareness with recall during general anesthesia: Incidence and risk factors. *Anesth. Analg.* **86**, 1084–1089 (1998).
27. R. H. Sandin, G. Enlund, P. Samuelsson, C. Lennmarken, Awareness during anaesthesia: A prospective case study. *Lancet* **355**, 707–711 (2000).
28. C. L. Errando *et al.*, Awareness with recall during general anaesthesia: A prospective observational evaluation of 4001 patients. *Br. J. Anaesth.* **101**, 178–185 (2008).
29. P. S. Myles, K. Leslie, J. McNeil, A. Forbes, M. T. V. Chan, Bispectral index monitoring to prevent awareness during anaesthesia: The B-Aware randomised controlled trial. *Lancet* **363**, 1757–1763 (2004).
30. M. S. Avidan *et al.*, Anesthesia awareness and the bispectral index. *N. Engl. J. Med.* **358**, 1097–1108 (2008).
31. M. S. Avidan *et al.*, Prevention of intraoperative awareness in high-risk surgical population. *N. Engl. J. Med.* **2011**, 591–600 (2011).
32. J. Wang *et al.*, Monitoring the end-tidal concentration of sevoflurane for preventing awareness during anesthesia (MEETS-PANDA): A prospective clinical trial. *Int. J. Surg.* **41**, 44–49 (2017).
33. L. Xu, A. S. Wu, Y. Yue, The incidence of intra-operative awareness during general anesthesia in China: A multi-center observational study. *Acta Anaesthesiol. Scand.* **53**, 873–882 (2009).
34. O. Chaiwat, K. Vacharaksa, U. Prakanrattana, Awareness under general anesthesia. *J. Med. Assoc. Thai.* **85**, 948–955 (2002).
35. C. Zhang *et al.*, Bispectral index monitoring prevent awareness during total intravenous anesthesia: A prospective, randomized, double-blinded, multi-center controlled trial. *Chin. Med. J. (Engl.)* **124**, 3664–3669 (2011).
36. G. A. Mashour *et al.*, Prevention of intraoperative awareness with explicit recall in an unselected surgical populationa randomized comparative effectiveness trial. *Anesthesiology* **117**, 717–725 (2012).
37. H. E. Braithwaite *et al.*, Impact of female sex on anaesthetic awareness, depth, and emergence: A systematic review and meta-analysis. *Br. J. Anaesth.* **131**, 510–522 (2023).
38. V. Erden *et al.*, Increased progesterone production during the luteal phase of menstruation may decrease anesthetic requirement. *Anesth. Analg.* **101**, 1007 (2005).
39. F. Fu *et al.*, Propofol EC50 for inducing loss of consciousness is lower in the luteal phase of the menstrual cycle. *Br. J. Anaesth.* **112**, 506–513 (2014).
40. L. Vutskits, J. D. Clark, E. D. Kharasch, Reporting laboratory and animal research in anesthesiologythe importance of sex as a biologic variable. *Anesthesiology* **131**, 949–952 (2019).
41. O. A. Moody, K. F. Vincent, K. Solt, Sex, drugs, and anaesthesia research. *Br. J. Anaesth.* **127**, 340–343 (2021).
42. S. M. Joksimovic *et al.*, Differential effects of the novel neurosteroid hypnotic (3β,5β,17β)-3-hydroxyandrostane-17-carbonitrile on electroencephalogram activity in male and female rats. *Br. J. Anaesth.* **127**, 435–446 (2021).
43. M. T. Mansouri, J. A. Fidler, Q. C. Meng, R. G. Eckenhoff, P. S. García, Sex effects on behavioral markers of emergence from propofol and isoflurane anesthesia in rats. *Behav. Brain Res.* **367**, 59–67 (2019).
44. Y. Zhang *et al.*, Estrogen receptor-A in medial preoptic area contributes to sex difference of mice in response to sevoflurane anesthesia. *Neurosci. Bull.* **38**, 703 (2022).
45. G. Fink *et al.*, Sex difference in response to alphaxalone anaesthesia may be oestrogen dependent. *Nature* **298**, 270–272 (1982).
46. K. F. Vincent *et al.*, Oestrous cycle affects emergence from anaesthesia with dexmedetomidine, but not propofol, isoflurane, or sevoflurane, in female rats. *Br. J. Anaesth.* **131**, 67–78 (2023).
47. B. S. McEwen, P. G. Davis, B. Parsons, D. W. Pfaff, The brain as a target for steroid hormone action. *Annu. Rev. Neurosci.* **2**, 65–112 (1979).
48. D. W. Pfaff, B. S. McEwen, Actions of estrogens and progestins on nerve cells. *Science* **219**, 808–814 (1983).

49. K. L. Maier *et al.*, Protocol for the reconstructing consciousness and cognition (ReCCognition) study. *Front. Hum. Neurosci.* **11**, 284 (2017).
50. A. Z. Wasilczuk, K. L. Maier, M. B. Kelz, The mouse as a model organism for assessing anesthetic sensitivity. *Methods Enzymol.* **602**, 211–228 (2018).
51. S. Gao, D. P. Calderon, Robust alternative to the righting reflex to assess arousal in rodents. *Sci. Rep.* **101**, 20280 (2020).
52. K. F. Vincent *et al.*, Return of the righting reflex does not portend recovery of cognitive function in anesthetized rats. *Front. Syst. Neurosci.* **15**, 762096 (2021).
53. A. R. McKinstry-Wu *et al.*, Analysis of stochastic fluctuations in responsiveness is a critical step toward personalized anesthesia. *eLife* **8**, e50143 (2019).
54. A. Z. Wasilczuk *et al.*, Resistance to state transitions in responsiveness is differentially modulated by different volatile anaesthetics in male mice. *Br. J. Anaesth.* **125**, 308–320 (2020).
55. A. Z. Wasilczuk, Q. C. Meng, A. R. McKinstry-Wu, Electroencephalographic evidence for individual neural inertia in mice that decreases with time. *Front. Syst. Neurosci.* **15**, 168 (2022).
56. B. P. Shortal *et al.*, Duration of EEG suppression does not predict recovery time or degree of cognitive impairment after general anaesthesia in human volunteers. *Br. J. Anaesth.* **123**, 206–218 (2019).
57. G. A. Mashour *et al.*, Recovery of consciousness and cognition after general anesthesia in humans. *eLife* **10**, e59525 (2021).
58. E. Gorczynska, D. J. Handelsman, Androgens rapidly increase the cytosolic calcium concentration in Sertoli cells. *Endocrinology* **136**, 2052–2059 (1995).
59. B. S. McEwen, Non-genomic and genomic effects of steroids on neural activity. *Trends Pharmacol. Sci.* **12**, 141–147 (1991).
60. M. E. Brocca, L. M. Garcia-Segura, Non-reproductive functions of aromatase in the central nervous system under physiological and pathological conditions. *Cell. Mol. Neurobiol.* **39**, 473–481 (2019).
61. A. Biegon, In vivo visualization of aromatase in animals and humans. *Front. Neuroendocrinol.* **40**, 42–51 (2016).
62. K. Takahashi *et al.*, Association between aromatase in human brains and personality traits. *Sci. Rep.* **8**, 16841 (2018).
63. C. E. Roselli, S. E. Abdelgadir, J. A. Resko, Regulation of aromatase gene expression in the adult rat brain. *Brain Res. Bull.* **44**, 351–357 (1997).
64. S. E. Abdelgadir *et al.*, Androgens regulate aromatase cytochrome P450 messenger ribonucleic acid in rat brain. *Endocrinology* **135**, 395–401 (1994).
65. C. E. Roselli, J. A. Resko, Testosterone regulates aromatase activity in discrete brain areas of male rhesus macaques1. *Biol. Reprod.* **40**, 929–934 (1989).
66. M. J. Kelly, O. K. Rønnekleiv, "45–Rapid membrane effects of estrogen in the central nervous system" in *Hormones, Brain and Behavior*, D. W. Pfaff, A. P. Arnold, S. E. Fahrbach, A. M. Etgen, R. T. Rubin, Eds. (Academic Press, 2002), pp. 361–380, 10.1016/B978-012532104-4/50047-0.
67. A. Proekt, Brief introduction to electroencephalography. *Methods Enzymol.* **603**, 257–277 (2018).
68. G. A. Mashour, Monitoring consciousness: EEG-based measures of anesthetic depth. *Semin. Anesth. Perioper. Med. Pain* **25**, 205–210 (2006).
69. R. Ní Mhuircheartaigh, C. Warnaby, R. Rogers, S. Jbabdi, I. Tracey, Slow-wave activity saturation and thalamocortical isolation during propofol anesthesia in humans. *Sci. Transl. Med.* **5**, 208ra148 (2013).
70. P. L. Purdon *et al.*, Electroencephalogram signatures of loss and recovery of consciousness from propofol. *Proc. Natl. Acad. Sci. U.S.A.* **110**, E1142–E1151 (2013).
71. A. Franceschini, I. Costantini, F. S. Pavone, L. Silvestri, Dissecting neuronal activation on a brain-wide scale with immediate early genes. *Front. Neurosci.* **14**, 569517 (2020).
72. Y. G. Park *et al.*, Protection of tissue physicochemical properties using polyfunctional crosslinkers. *Nat. Biotechnol.* **371**, 73–83 (2018).
73. S. Y. Kim *et al.*, Stochastic electrotransport selectively enhances the transport of highly electromobile molecules. *Proc. Natl. Acad. Sci. U.S.A.* **112**, E6274–E6283 (2015).
74. E. Murray *et al.*, Simple, scalable proteomic imaging for high-dimensional profiling of intact systems. *Cell* **163**, 1500–1514 (2015).
75. E. Shelhamer, J. Long, T. Darrell, Fully convolutional networks for semantic segmentation. *IEEE Trans. Pattern Anal. Mach. Intell.* **39**, 640–651 (2016).
76. K. He, X. Zhang, S. Ren, J. Sun, "Deep residual learning for image recognition" in *2016 IEEE Conference on Computer Vision and Pattern Recognition (CVPR)*, (IEEE Computer Society, Los Alamitos, CA, 2016), pp. 770–778, 2016-December.
77. Q. Wang *et al.*, The allen mouse brain common coordinate framework: A 3D reference atlas. *Cell* **181**, 936–953.e20 (2020).
78. D. F. Swaab, E. Fliers, A sexually dimorphic nucleus in the human brain. *Science* **228**, 1112–1115 (1985).
79. Y. Tsuneoka, H. Funato, Cellular composition of the preoptic area regulating sleep, parental, and sexual behavior. *Front. Neurosci.* **15**, 649159 (2021).
80. R. Szymusiak, I. Gvilia, D. McGinty, Hypothalamic control of sleep. *Sleep Med.* **8**, 291–301 (2007).
81. M. B. Kelz, G. A. Mashour, The biology of general anesthesia from paramecium to primate. *Curr. Biol.* **29**, R1199–R1210 (2019).
82. L. E. Nelson *et al.*, The sedative component of anesthesia is mediated by GABA(A) receptors in an endogenous sleep pathway. *Nat. Neurosci.* **5**, 979–984 (2002).
83. B. Han, H. S. McCarren, D. O'Neill, M. B. Kelz, Distinctive recruitment of endogenous sleep-promoting neurons by volatile anesthetics and a nonimmobilizer. *Anesthesiology* **121**, 999–1009 (2014).
84. J. Lu *et al.*, Role of endogenous sleep-wake and analgesic systems in anesthesia. *J. Comp. Neurol.* **508**, 648–662 (2008).
85. Z. Xu *et al.*, Corticotropin-releasing factor neurones in the paraventricular nucleus of the hypothalamus modulate isoflurane anaesthesia and its responses to acute stress in mice. *Br. J. Anaesth.* **130**, 446–458 (2023).
86. S. L. Reitz, A. Z. Wasilczuk, G. H. Beh, A. Proekt, M. B. Kelz, Activation of preoptic tachykinin 1 neurons promotes wakefulness over sleep and volatile anesthetic-induced unconsciousness. *Curr. Biol.* **31**, 394–405.e4 (2021).
87. M. B. Kelz *et al.*, An essential role for orexins in emergence from general anesthesia. *Proc. Natl. Acad. Sci. U.S.A.* **105**, 1309–1314 (2008).
88. H. Dong *et al.*, Activation of orexin signal in basal forebrain facilitates the emergence from sevoflurane anesthesia in rat. *Neuropeptides* **43**, 179–185 (2009).
89. J. R. Moffitt *et al.*, Molecular, spatial, and functional single-cell profiling of the hypothalamic preoptic region. *Science* **362**, eaau5324 (2018).
90. M. V. Wu *et al.*, Estrogen masculinizes neural pathways and sex-specific behaviors. *Cell* **139**, 61–72 (2009).
91. M. Joëls, R. A. Sarabdjitsingh, H. Karst, Unraveling the time domains of corticosteroid hormone influences on brain activity: Rapid, slow, and chronic modes. *Pharmacol. Rev.* **64**, 901–938 (2012).
92. H. C. Hemmings *et al.*, Towards a comprehensive understanding of anesthetic mechanisms of action: A decade of discovery. *Trends Pharmacol. Sci.* **40**, 464–481 (2019).
93. G. Akk *et al.*, Mechanisms of neurosteroid interactions with GABAA receptors. *Pharmacol. Ther.* **116**, 35–57 (2007).
94. D. Belelli, J. J. Lambert, Neurosteroids: Endogenous regulators of the GABAA receptor. *Nat. Rev. Neurosci.* **6**, 565–575 (2005).
95. D. Belelli, M. Pistis, J. A. Peters, J. J. Lambert, The interaction of general anaesthetics and neurosteroids with GABAA and glycine receptors. *Neurochem. Int.* **34**, 447–452 (1999).
96. M. M. McCarthy, A. P. Auger, T. S. Perrot-Sinal, Getting excited about GABA and sex differences in the brain. *Trends Neurosci.* **25**, 307–312 (2002).
97. S. C. Piantadosi *et al.*, Sex-dependent anti-stress effect of an α5 subunit containing GABAA receptor positive allosteric modulator. *Front. Pharmacol.* **7**, 446 (2016).
98. F. A. Gibbs, E. L. Gibbs, W. G. Lennox, Effect on the electro-encephalogram of certain drugs which influence nervous activity. *Arch. Intern. Med.* **60**, 154–166 (1937).
99. D. Chander, P. S. García, J. N. MacColl, S. Illing, J. W. Sleigh, Electroencephalographic variation during end maintenance and emergence from surgical anesthesia. *PLoS One* **9**, e106291 (2014).
100. D. F. Hight *et al.*, Emergence from general anesthesia and the sleep-manifold. *Front. Syst. Neurosci.* **8**, 146 (2014).
101. C. E. Warnaby, J. W. Sleigh, D. Hight, S. Jbabdi, I. Tracey, Investigation of slow-wave activity saturation during surgical anesthesia reveals a signature of neural inertia in humans. *Anesthesiology* **127**, 645–657 (2017).
102. G. Schneider *et al.*, Bispectral Index (BIS) may not predict awareness reaction to intubation in surgical patients. *J. Neurosurg. Anesthesiol.* **14**, 7–11 (2002).
103. I. F. Russell, The Narcotrend 'depth of anaesthesia' monitor cannot reliably detect consciousness during general anaesthesia: An investigation using the isolated forearm technique. *Br. J. Anaesth.* **96**, 346–352 (2006).
104. B. Kocaman Akbay, Y. Demiraran, G. Yalcin Sezen, G. Akcali, A. Somunkiran, Use of the bispectral index to predict a positive awareness reaction to laryngeal mask airway–Fastrach insertion and intubation. *Acta Anaesthesiol. Scand.* **51**, 1368–1372 (2007).
105. I. F. Russell, The ability of bispectral index to detect intra-operative wakefulness during total intravenous anaesthesia compared with the isolated forearm technique. *Anaesthesia* **68**, 502–511 (2013).
106. I. F. Russell, The ability of bispectral index to detect intra-operative wakefulness during isoflurane/air anaesthesia, compared with the isolated forearm technique. *Anaesthesia* **68**, 1010–1020 (2013).
107. F. Zand, S. M. R. Hadavi, A. Chohedri, P. Sabetian, Survey on the adequacy of depth of anaesthesia with bispectral index and isolated forearm technique in elective Caesarean section under general anaesthesia with sevoflurane. *BJA Br. J. Anaesth.* **112**, 871–878 (2014).
108. R. D. Sanders *et al.*, Incidence of connected consciousness after tracheal intubation: A prospective, international, multicenter cohort study of the isolated forearm technique. *Anesthesiology* **126**, 214–222 (2017).
109. F. Linassi, P. Zanatta, P. Tellaroli, C. Ori, M. Carron, Isolated forearm technique: A meta-analysis of connected consciousness during different general anaesthesia regimens. *Br. J. Anaesth.* **121**, 198–209 (2018).
110. Y. Sun *et al.*, High throughput modular chambers for rapid evaluation of anesthetic sensitivity. *BMC Anesthesiol.* **6**, 13 (2006).
111. A. Z. Wasilczuk, A. Proekt, M. B. Kelz, A. R. McKinstry-Wu, High-density electroencephalographic acquisition in a rodent model using low-cost and open-source resources. *J. Vis. Exp.* **117**, e54908 (2016), 10.3791/54908.
112. J. H. Siegle *et al.*, Open Ephys: An open-source, plugin-based platform for multichannel electrophysiology. *J. Neural Eng.* **14**, 045003 (2017).
113. A. E. Hudson, D. P. Calderon, D. W. Pfaff, A. Proekt, Recovery of consciousness is mediated by a network of discrete metastable activity states. *Proc. Natl. Acad. Sci. U.S.A.* **111**, 9283–9288 (2014).
114. A. Aggarwal *et al.*, Coherence of visual-evoked gamma oscillations is disrupted by propofol but preserved under equipotent doses of isoflurane. *Front. Syst. Neurosci.* **13**, 19 (2019).
115. M. Basner *et al.*, Development and validation of the Cognition test battery for spaceflight. *Aerosp. Med. Hum. Perform.* **86**, 942–952 (2015).
116. M. Basner, D. F. Dinges, Maximizing sensitivity of the psychomotor vigilance test (PVT) to sleep loss. *Sleep* **34**, 581–591 (2011).
117. M. Basner, D. Mollicone, D. F. Dinges, Validity and sensitivity of a brief psychomotor vigilance test (PVT-B) to total and partial sleep deprivation. *Acta Astronaut.* **69**, 949–959 (2011).
118. W. A. Wickelgren, Speed-accuracy tradeoff and information processing dynamics. *Acta Psychol. (Amst.)* **41**, 67–85 (1977).
119. J. A. Hartigan, P. M. Hartigan, The dip test of unimodality. *Ann. Stat.* **13**, 70–84 (1985).
120. P. C. Austin, J. E. Hux, A brief note on overlapping confidence intervals. *J. Vasc. Surg.* **36**, 194–195 (2002).
121. A. Aggarwal *et al.*, Visual evoked feedforward–feedback traveling waves organize neural activity across the cortical hierarchy in mice. *Nat. Commun.* **13**, 4754 (2022).